Research Article

α-Si_3N_4 and Si_2N_2O whiskers from rice husk and industrial rice husk ash

A. Parrillo[1] · G. Sánchez[1] · A. Bologna Alles[1]

Received: 4 September 2020 / Accepted: 29 January 2021 / Published online: 3 February 2021

Abstract
Rice industrialization worldwide generates significant amounts of rice husk as a by-product. When rice husk is burned to obtain energy, a relatively common practice, a substantial portion of the husk turns into ash, and both constitute environmental liabilities. Using rice husk and ash as starting materials to produce high-value products could help in mitigating the environmental impact while providing economic revenue. Rice husk and rice husk ash as produced in a local cogeneration plant without any pretreatments were evaluated as feasible sources for silicon nitride (Si_3N_4) and silicon oxynitride (Si_2N_2O) whiskers by carbothermal reduction and nitridation. Rice husk and the ash were held at temperatures between 1200 and 1400 °C for 3 h under flowing nitrogen. Increasing soaking temperature values led to higher whisker development for both starting materials, with the best results observed at 1400 °C. Whereas α-silicon nitride whiskers were obtained when rice husk was employed, the graphite surface-to-ash ratio dictated whisker composition for the ash. Treatment of the ash at the soaking temperature value of 1400 °C led to silicon oxynitride for lower graphite surface-to-ash ratios, but when this ratio was increased, α-silicon nitride predominated. α-silicon nitride whiskers had cross sections ranging from about 100 nm to 1 μm in width, whereas the silicon oxynitride whiskers had cross sections ranging from approx. 100 to 500 nm in diameter. Both types of whiskers were observed to be in the millimeter length range.

Keywords Rice husk · Rice husk ash · Silicon nitride · Silicon oxynitride · Whiskers · Carbothermal reduction and nitridation

1 Introduction

Rice husk accounts for nearly 20% of the weight of paddy grain and is the main waste associated with the rice mill industry. Rice husk usually contains close to 80% organic matter: 35% cellulose, 25% hemicellulose, and 20% lignin approximately. The inorganic fraction, mainly silica, accounts for roughly 20% of the husk mass [1]. Hence, when rice husk is burned, usually to generate energy, large amounts of ash are produced.

One option to mitigate the environmental impact of the waste disposal and at the same time add value to the husk and the ash could be found by using these to produce high-value ceramic materials. Rice husk and rice husk ash can be used as an alternative source of silica in both traditional and advanced ceramics [2–5]. The intimate contact of silica and carbon found in rice husk and rice husk ash makes these residues promising for the synthesis of various products. Under suitable conditions, carbothermal reduction of silica leads to silicon carbide (SiC) [6–8], while carbothermal reduction of silica followed by nitridation results in silicon nitride [7], and some reports indicate silicon oxynitride as well [9].

Silicon nitride is an insulator with covalent bonding [6]. It has high mechanical strength even at elevated temperatures, high-temperature corrosion and superior thermal shock resistance, and high toughness when compared to other ceramic materials [7]. It is used in refractories, as well as in cutting tools and bearings, and it is added as whiskers to reinforce metals and ceramic matrixes [10].

✉ A. Parrillo, aparrillo@fing.edu.uy | [1]Departamento Ingeniería de Materiales y Minas, Facultad de Ingeniería – UdelaR, Instituto de Ingeniería Química, Julio Herrera y Reissig 565, 11300 Montevideo, Uruguay.

Silicon nitride occurs mainly in two hexagonal close-packed structures, a trigonal α-form stable at lower temperatures, and a hexagonal β-form observed at higher temperatures. Both the α- and β-phases are formed by slightly distorted SiN_4 tetrahedra sharing nitrogen atoms at the corners, but they differ in their stacking sequence. α-silicon nitride is typically preferred as the starting material for sintered parts because of its higher solubility in the liquid phase formed by the additives used to promote densification [7].

Silicon oxynitride also presents a fair degree of covalent bonding and is a refractory material with high chemical and oxidation resistance. Its rhombohedral crystalline structure is formed by SiN_3O tetrahedra sharing all corners, connected through oxygen atoms along the c axis, and by nitrogen atoms in the perpendicular directions [8].

Whiskers, single-crystal-like fibers with diameters in the micrometer range and high aspect ratios, have fewer flaws due to their small size and the absence of high-angle grain boundaries. As a result, they can exhibit strengths close to theoretical values. Ceramic whiskers may be added to metal matrixes to enhance their strength, and to ceramic matrixes for strengthening and toughening purposes [10].

There are different works on the synthesis of silicon carbide starting from rice husk, pyrolyzed rice husk, or rice husk ash prepared under laboratory conditions [10]. Works focusing on silicon nitride and silicon oxynitride production are less frequent, and in most cases, rice husk pretreatments were usually employed, where grinding [11], pyrolysis [12], digestion in acid solutions [13], and other similar methods [9, 10, 12, 14–24] have been used. Pretreatments pose a burden and additional costs to an industrial operation.

There are even fewer references reporting the use of rice husk ash coming from an industrial combustion process [25, 26]. The conditions used in the industrial combustion process regulate important ash parameters, such as carbon-to-silica content ratio, specific surface area, and silica crystallinity [1], and some variability should be expected among the ashes produced in different cogeneration plants.

Carbothermal reduction requires a carbon source and a metal oxide, while high temperatures are needed to move along the overall process to completion. Higher temperature values promote some of the key forward reactions due to their high endothermic natures [7], while at the same time, the formation of some important gaseous intermediaries is fostered as well.

The carbothermal reduction and nitridation reactions to produce silicon nitride and silicon oxynitride indicate that the stoichiometric carbon-to-silica molar ratio for silicon nitride is 2, whereas for silicon oxynitride is 1.5 (see Eqs. 1 and 2):

$$3SiO_{2(S)} + 6C_{(s)} + 2N_{2(g)} \leftrightarrow Si_3N_{4(s)} + 6CO_{(g)} \quad (1)$$

$$2SiO_{2(g)} + 3C_{(s)} + N_{2(g)} \leftrightarrow Si_2N_2O_{(s)} + 3CO_{(g)} \quad (2)$$

This work aimed to evaluate the feasibility and the best experimental setup to produce silicon nitride and silicon oxynitride whiskers through carbothermal reduction and nitridation of as-received rice husk and rice husk ash coming from a local cogeneration plant without pretreatments or additions. The carbon source needed to react with the silica in both starting materials was provided only by the organic matter already present in the husk and the ash, with no extra carbon added as a reactant**.**

The dry-basis loss on ignition (LOI) for the industrial rice husk ash used was found to be 10.2%. This value, although significantly lower than that of the husk, still makes a partial carbothermal reduction seem feasible since the carbon-to-silica molar ratio can be roughly estimated to be around a value of 0.6, assuming the inorganic material to be silica and the LOI as carbon.

2 Experimental procedure

Rice husk from mills located in the eastern portion of Uruguay and rice husk ash produced by a local cogeneration plant that operates burning husk were used as starting materials. After drying to constant weight at 105 °C, particle-size distributions were determined for the husk and the ash, and LOI tests were conducted on both starting materials. X-ray fluorescence (XRF) and wet-chemical analysis were conducted on LOI-test residues to assess elemental chemical composition.

For carbothermal reduction and nitridation, samples were loaded in graphite (ELLOR®, density = 1.9 g/cm^3) and alumina (99.8% aluminum oxide) crucibles with lids in various configurations and introduced in the furnace. The system was then evacuated to 1 Pa, and N_2 gas (min. 99.9% N_2) was allowed to flow at 0.2 L/min for all the runs while heating and cooling. The furnace was ramped at 6 °C/min to the selected temperature of the run, soaked for 180 min, and then allowed to cool at 5 °C/min to 200 °C, followed by furnace cooling. The samples were soaked at 1200 °C, 1250 °C, 1320 °C, and 1400 °C in graphite crucibles. Other crucible configurations, varying the crucible material and the lid setup, were tested at 1400 °C.

The starting materials and products were characterized by scanning electron microscopy (SEM—JEOL JSM-5900LV) fitted with energy-dispersive X-ray spectroscopy (EDS). Standard $\theta - 2\theta$ X-ray diffraction (XRD—Philips PW180—30 kV—40 mA, Cu Kα radiation $\lambda = 1.5406$ Å) pattern analysis was conducted on the starting materials and

on the whiskers found to be deposited on the crucible surfaces after the furnace runs.

Fourier transformed infrared spectroscopy (FTIR—Shimadzu IRAffinity-1S) was used on both raw materials and on the whiskers deposited on the crucible surfaces after the furnace runs. Pellets formed using KBr with dry rice husk and ash were analyzed by a transmission technique, while attenuated total reflection was used on the whiskers produced after the furnace runs.

3 Results and discussion

3.1 Rice husk and rice husk ash characterization

The as-received rice husk ash, although more fragmented, retains somewhat a similar structure to the one found in the husk, and some insufficiently burned husk portions can be observed in the ash as well (see Fig. 1). The granulometric analysis revealed that the starting materials mean particle size was 1.4 mm for the husk and 0.25 mm for the ash.

XRD and FTIR patterns of the starting materials are shown in Fig. 2. Both XRD patterns exhibit a peak at $2\theta = 22°$ indicating the presence of relatively amorphous cristobalite, where a sharper peak can be observed in the industrial ash suggesting that the silica present in the ash could have a higher degree of crystallinity when compared to the husk. Also, an incipient peak corresponding to cristobalite can be observed in the ash at $2\theta = 36.5°$ that it is not present in the husk (see Fig. 2).

The FTIR spectrum for rice husk (see Fig. 2) exhibits bands consistent with the presence of organic matter—cellulose, hemicellulose, and lignin—together with the presence of silica as well. The 3700–3000 cm^{-1} broad IR band suggests the presence of hydroxyl groups, while the 3000–2800 cm^{-1} band is consistent with methylene functional groups, and other lower frequency bands are probably due to carboxylic, aromatic double bonds, and methylene groups [27].

The IR bands centered at 1100 cm^{-1}, 790 cm^{-1}, 617 cm^{-1}, and 470 cm^{-1} can be attributed to the presence of silica [28]. Upon inspection, the rice husk ash spectrum indicates that inorganic components are more predominant when compared to the spectrum of the husk (see Fig. 2).

The elemental chemical analysis for rice husk and the industrial ash is presented in Table 1.

If the LOI is taken to be cellulose for the husk and carbon for the ash, the carbon-to-silica molar ratios can be estimated as 9.1 for the husk and 0.6 for the ash. However, the organic matter in rice husk is partially lost upon heating since carbothermal reduction and nitridation reactions do not truly begin with appreciable rates up to high temperatures; thus, the carbon-to-silica ratio for the husk under reaction conditions should be different from the initial ratio of 9.1.

To estimate the actual carbon-to-silica ratio when the process reactions in the furnace begin to take place, rice

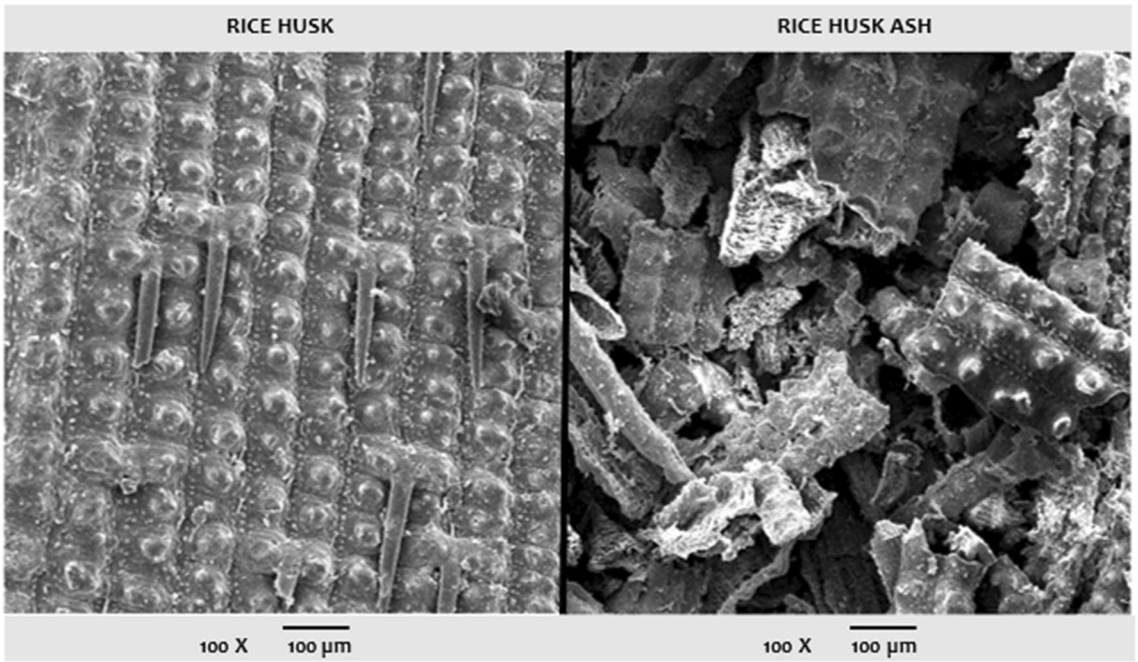

Fig. 1 SEM SE images of the as-received rice husk and rice husk ash

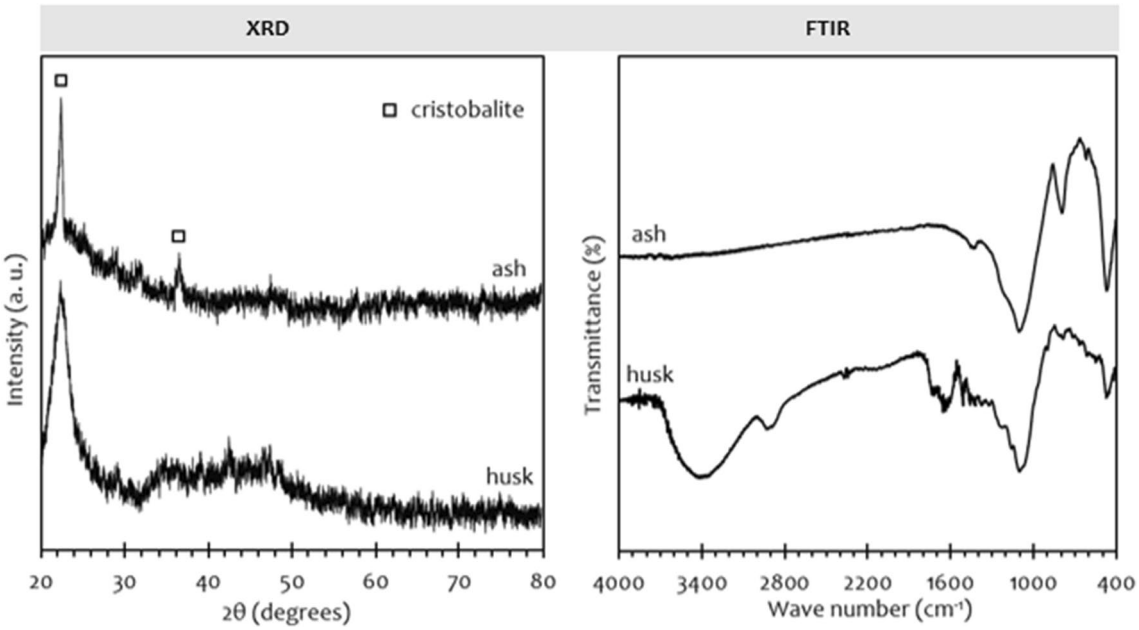

Fig. 2 XRD and FTIR patterns of the as-received rice husk and rice husk ash

Table 1 Assayed elemental chemical compositions of the as-received rice husk and industrial ash

Composition (wt%)	LOI	SiO_2	K_2O	CaO	Fe_2O_3	P_2O_5	MnO_2	Na_2O
Rice husk	79.8	19.3	0.31	0.15	0.02	0.24	0.07	0.02
Industrial ash	10.2	86.1	0.99	0.77	0.09	0.91	0.40	0.13

husk was ramped up to 1200 °C under the same conditions as the experimental runs and immediately cooled down without allowing the samples to remain at the soaking step. No observable carbothermal reaction was apparent after this run; however, the husk was partially pyrolyzed as a result. The dry-basis LOI of the leftover pyrolyzed material was found to be 47%, which is comparatively lower than the starting value of 79.8%.

If all the inorganic material remaining after this test run is assumed to be silica and the LOI due to carbon, the effective carbon-to-silica molar ratio in the husk can be now estimated to be 4.4, indicating that a fair excess of carbon in the husk remains up to 1200 °C, and this value is still substantially higher than the effective carbon-to-silica ratio value of 0.6 found in the ash.

3.2 Soaking temperature

3.2.1 Rice husk

Carbothermal reduction and nitridation of the husk at a soaking temperature value of 1200 °C produced almost no whiskers. A more substantial whisker development was observed for the run at 1250 °C, while the material left at the bottom of the crucible appeared to be significantly more pyrolyzed. The whiskers were found almost entirely deposited on the crucible and lid internal surfaces rather than on the residue leftover from the starting material (see Fig. 3).

Under increasing soaking temperature values, i.e., 1320 °C and 1400 °C, more whiskers developed, and while whisker growth was chiefly found on the crucible walls and lids, some growth was also observed on the material residue left at the bottom of the crucible. Moreover, a significant increase in both length and diameter of the whiskers resulted in the run at 1400 °C, suggesting that a full-fledged reaction had taken place under the latter conditions (see Figs. 3, 4, 5).

The silicon nitride whiskers obtained had lengths in the millimeter range with cross sections ranging from about 100 nm up to 1 μm for the different runs (see Figs. 4, 5). While the more developed whiskers exhibited square or rectangular cross sections fitting to their crystal structure, the finer ones seemed to be rounder in shape, although their small size prevents better definition.

The FTIR spectra (see Fig. 6) of the whiskers deposited on the crucibles at 1250 °C, 1320 °C, and 1400 °C exhibit the typical IR bands—922 cm^{-1}, 901 cm^{-1}, 882 cm^{-1},

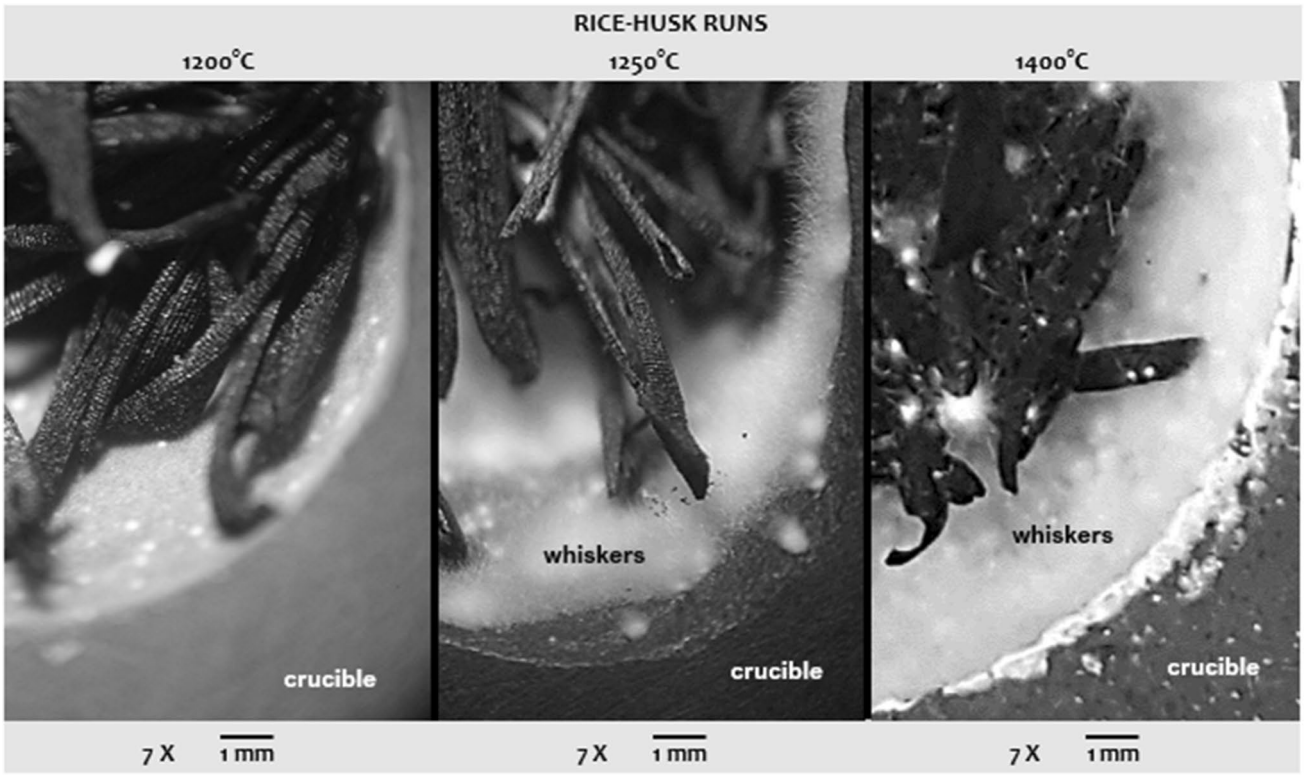

Fig. 3 Optical micrographs of rice husk runs in graphite crucibles at 1200 °C, 1250 °C, and 1400 °C

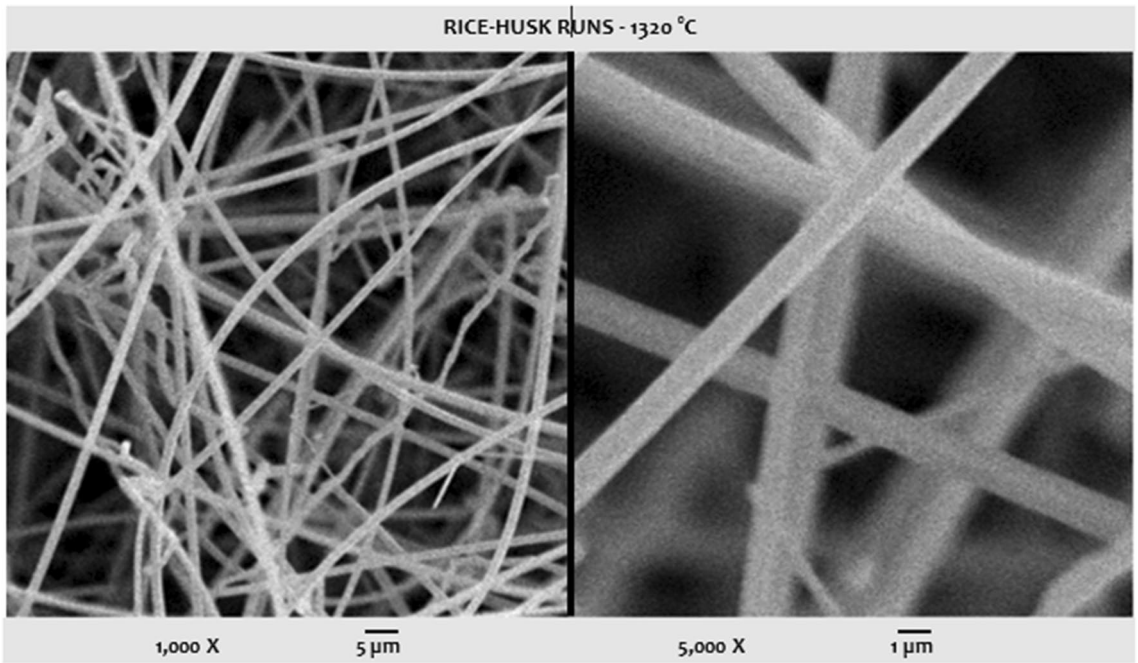

Fig. 4 SEM SE micrographs of silicon nitride whiskers obtained from rice husk in graphite crucibles at 1320 °C

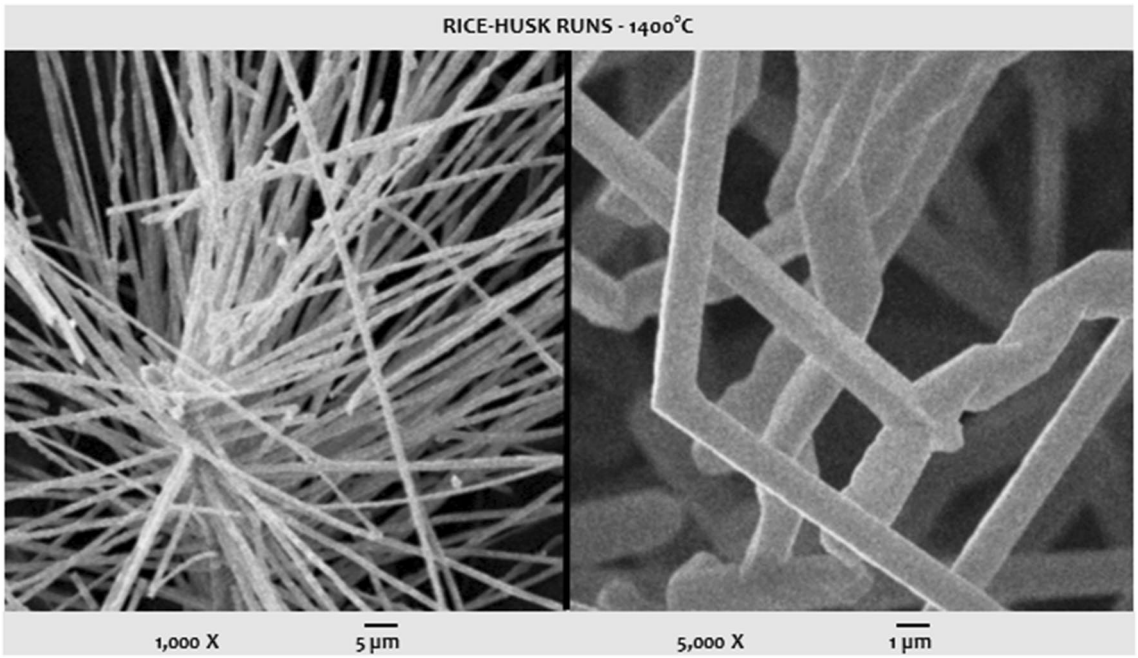

Fig. 5 SEM SE images of α-Si_3N_4 whiskers developed from rice husk in graphite crucibles at 1400 °C. A 120° angle can be observed for the change in the direction for the crystal growth following suit to the α-Si_3N_4 trigonal crystal system

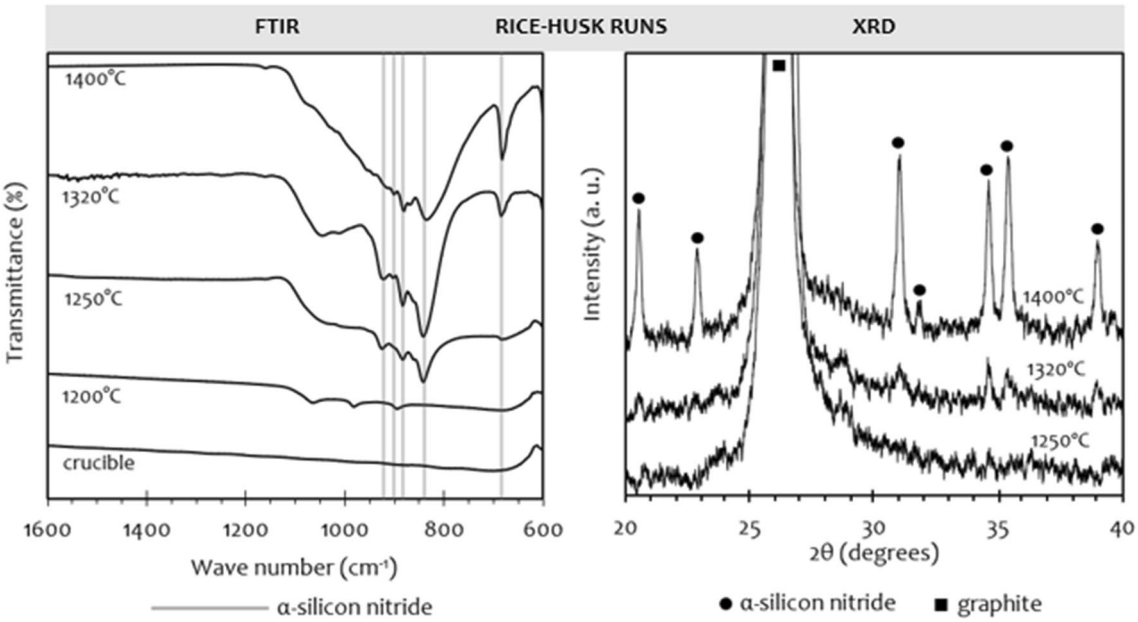

Fig. 6 FTIR spectra and XRD patterns of whiskers deposited on graphite crucibles for rice husk runs at increasing soaking temperature values. The FTIR spectrum of the as-was crucible was included for comparison purposes

840 cm^{-1}, and 683 cm^{-1}—compatible with the presence of α-Si_3N_4 [29]. However, a better developed and more closely resembling pattern can be observed for the run at 1400 °C. No characteristic nitride or oxynitride IR bands could be observed in the rather small amount of the whisker-like material found for the furnace run at 1200 °C (see Fig. 6).

The XRD patterns of the whisker deposits indicate the presence of α-Si_3N_4 on the crucible when the husk was treated at 1400 °C, with peaks at $2\theta = 31.1°$, 34.6°, 35.2°, and 39.2° (see Fig. 6) [30]. For the intermediate temperatures, 1250 °C and 1320 °C, only some incipient peaks are insinuated for the run at 1320 °C, suggesting similarly to

the FTIR spectra of these two runs, that the better results are achieved at the higher temperature value tested.

The results obtained here are in agreement with those found elsewhere [11, 23], although the methodology of the present work did not include rice husk pretreatments.

3.2.2 Rice husk ash

While no discernible whiskers were observed to develop when the industrial ash was held at the soaking temperature value of 1200 °C, a small amount of whiskers was obtained on the graphite crucible and lid surfaces at 1250 °C. The crucible inner surfaces were covered by a layer of white whiskers for the run at 1320 °C, while for the run at 1400 °C there was a marked development of whiskers on the crucible graphite surfaces, as well as some whisker growth on the residual material leftover in the bottom of the crucible (see Fig. 7).

Once again, a more vigorous reaction appeared to have taken place for the latter condition, although whisker growth was comparatively smaller than the one observed for the husk. The whiskers obtained had diameters ranging from about 100 to 500 nm and lengths in the millimeter range (see Fig. 8); however, these were somewhat shorter than the α-silicon nitride whiskers obtained from the husk at the same temperature.

For the run at 1400 °C, the FTIR spectrum of the whiskers deposited on the graphite crucible and lid surfaces exhibits the characteristic IR bands—1070 cm^{-1}, 982 cm^{-1}, 938 cm^{-1}, 893 cm^{-1}, and 677 cm^{-1}—compatible with the presence of Si_2N_2O (see Fig. 9) [31]. It has been previously reported [25] that an oxynitride derivative was obtained from an industrial rice husk ash-derived material, although the final product described significantly differed from Si_2N_2O due to important compositional differences between the starting materials employed.

For the runs at 1320 °C and 1250 °C, some of the Si_2N_2O characteristic IR bands—primarily 1070 cm^{-1}, 982 cm^{-1}, and 893 cm^{-1}—can also be observed in the FTIR spectra of the whiskers, although these spectra do not completely resemble that of pure and stoichiometric Si_2N_2O. This may suggest that the whisker deposits obtained at intermediate temperature values may be somewhat chemically different from fully stoichiometric silicon oxynitride. Particularly, the much higher intensity of the 1070 cm^{-1} band for the runs at 1250 °C and 1320 °C, when compared to the one observed for the run at 1400 °C, may suggest that the compounds obtained at the intermediate temperatures might be oxygen rich since this frequency can be associated with the presence of Si–O bonds.

The XRD diffractograms were consistent with the FTIR spectra obtained (see Fig. 9). For 1400 °C, the XRD results

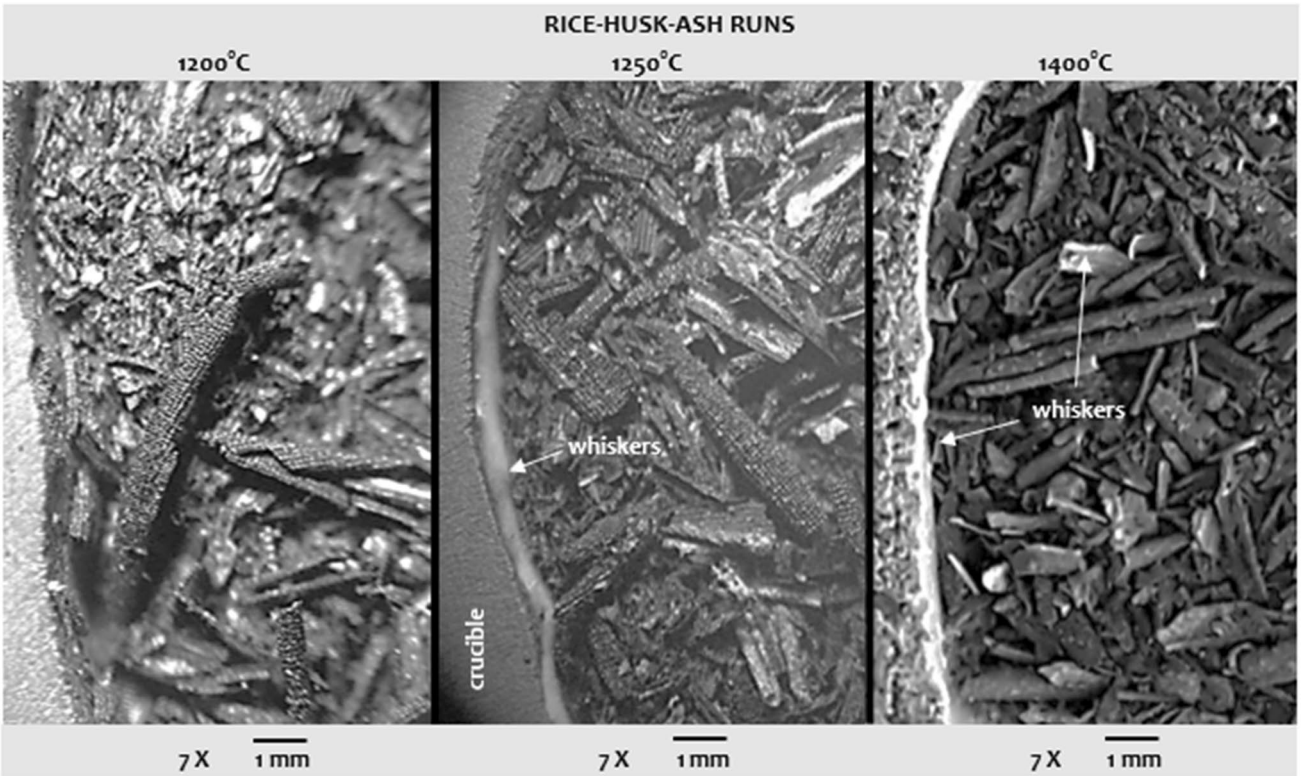

Fig. 7 Optical micrographs of rice husk ash runs in graphite crucibles at 1200 °C, 1250 °C, and 1400 °C

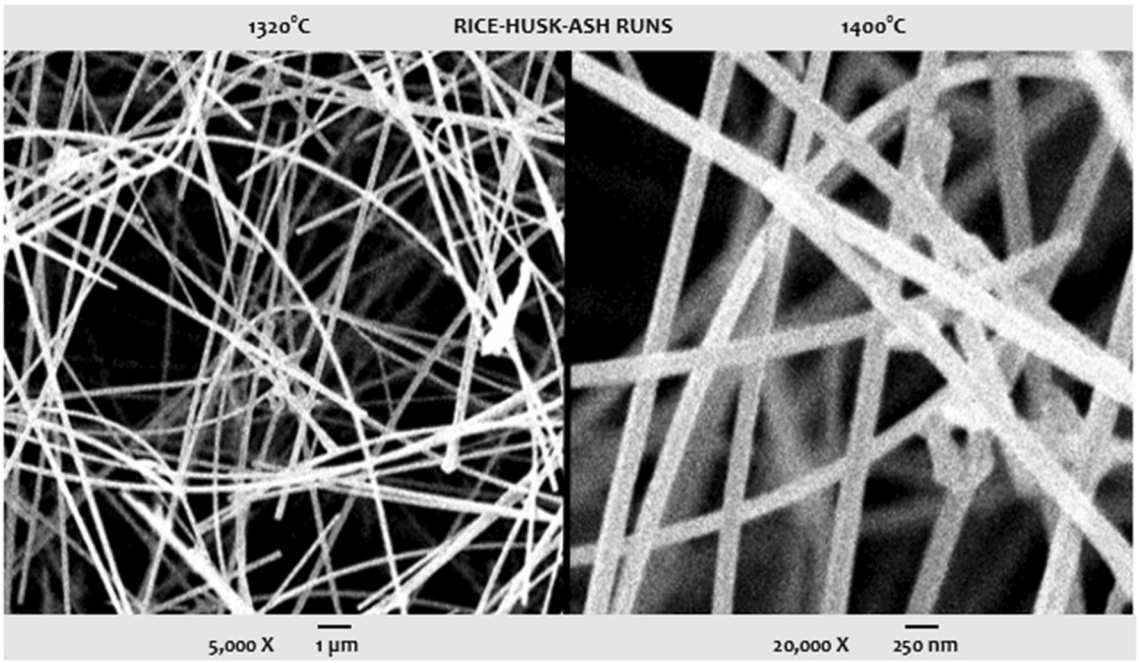

Fig. 8 SEM SE images of whiskers developed from industrial rice husk ash in graphite crucibles for the runs at 1320 °C and 1400 °C

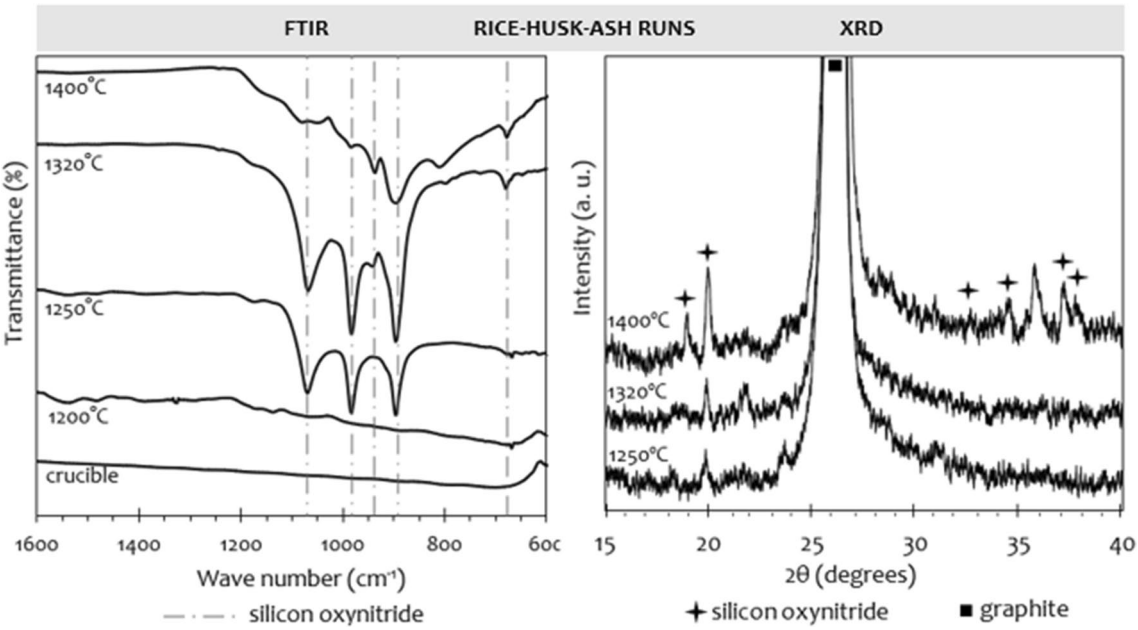

Fig. 9 FTIR spectra and XRD patterns of whiskers deposited on graphite crucibles for rice husk ash runs at increasing soaking temperature values. The FTIR spectrum of the as-was crucible was included for comparison purposes

confirmed the development of Si_2N_2O whiskers on the crucible with characteristic peaks at $2\theta = 19.1°$, 20.1°, 32.7°, 34.5°, 37.1°, and 37.7° [32], while the XRD spectra for 1320 °C and 1250 °C show only incipient peaks at the Si_2N_2O most intense reflection, namely 20.1°.

3.3 Crucible effect

3.3.1 Rice husk

Throughout the different runs, whiskers grew preferentially

on the surfaces of the graphite crucible and lid (see Fig. 3) when compared to the residue leftover from the starting material. To discern the importance of the presence of graphite in the reaction chamber on the overall reaction and crystallization process, two configurations were employed, namely alumina crucibles with alumina lids and alumina crucibles with graphite lids.

When alumina crucibles and lids were used with rice husk, a glassy phase formed that firmly sealed the lid to the crucible, and very little to no whisker production was observed, although the husk appeared to be thermally degraded, nonetheless. The presence of alkaline and alkaline-earth elements (see Table 1) in the husk possibly promoted the formation of the glassy phase responsible for the occlusion observed.

It was speculated that the seal prevented the necessary gas exchange required for the reactions to proceed, in particular the release of $CO_{(g)}$, is crucial for the carbothermal reduction step to move forward (see Eq. 3). The effect of $N_{2(g)}$ reaching the starting material was believed to be not as significant, considering that the prevailing conditions in the absence of nitrogen could have led to the production of silicon carbide whiskers, and no whisker development was indeed observed (see Eq. 4):

$$SiO_{2(s)} + C_{(s)} \leftrightarrow SiO_{(g)} + CO_{(g)} \quad (3)$$

$$SiO_{2(s)} + 3C_{(s)} \leftrightarrow SiC_{(s)} + 2CO_{(g)} \quad (4)$$

A different setup was therefore used, where just a small opening was left between the alumina crucibles and lids to allow for the needed gaseous exchange. For this new setup, also a glassy phase formed through the crucible and lid surfaces that were in contact; however, a good number of whiskers developed on the crucible and lid surfaces, as well as on the residual material left at the bottom of the crucible. In any case, the whisker amount produced was significantly smaller when compared to the setup employing graphite crucible and lids.

When alumina crucibles were fully closed using graphite lids, whisker development was comparable to the one found for the graphite crucible and lid configuration, with whiskers growing mainly on both the alumina crucible walls and on the graphite lid.

Figure 10 shows the FTIR spectra for all runs at 1400 °C starting from rice husk and rice husk ash resulting from all the different crucible setups. The FTIR spectra show that the whiskers deposited on the crucible surfaces for the three configurations where rice husk was used exhibited the characteristic IR bands—922 cm^{-1}, 901 cm^{-1}, 882 cm^{-1}, 840 cm^{-1}, and 683 cm^{-1}—compatible with the presence of α-Si_3N_4 [29].

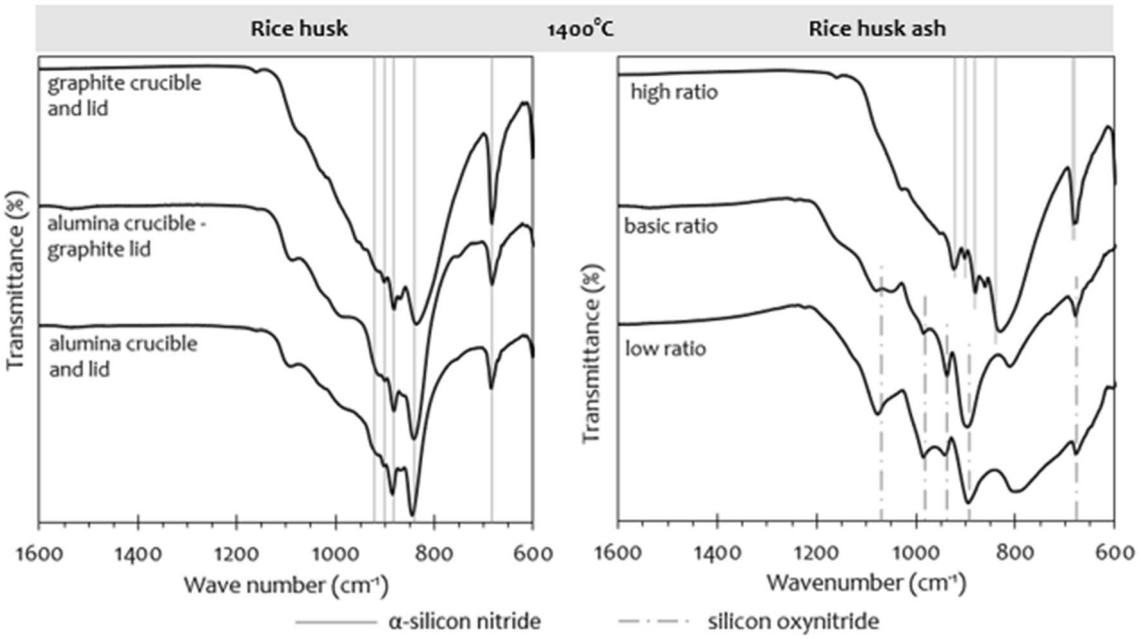

Fig. 10 FTIR spectra of the whiskers developed from rice husk and rice husk ash at a soaking temperature value of 1400 °C for different crucible setups. Rice husk in partially open alumina crucibles, alumina crucibles and graphite lids, and in all-graphite setups (left). Rice husk ash in graphite crucibles at different graphite surface-to-ash ratios: low ratio, basic ratio, and high ratio (right)

3.3.2 Rice husk ash

To elucidate if the graphite surface-to-ash ratio had a sizable effect, two additional configurations were used with a lower and a higher ratio compared to the standard one used in earlier runs, where an all-alumina crucible setup was also tested. Table 2 summarizes the results observed.

Similar to the husk setup, the alumina crucible and lid setup was implemented with a small opening. For this new setup, also a glassy phase formed through the crucible and lid surfaces that were in contact. Even though the opening allowed proper gaseous exchange, no whiskers were observed.

When the lower graphite crucible surface-to-ash ratio setups were used, comparatively more sample was placed on the crucible, and Si_2N_2O whiskers were produced, while α-Si_3N_4 whiskers resulted when a higher surface-to-ash ratio setup was employed (see Fig. 10). This suggests that the presence of graphite in sufficient amounts in contact with the ash can be considered to be a decisive factor in the development, as well as the final chemical composition, of whiskers produced from rice husk ash.

Table 2 Summary of all rice husk ash runs at 1400 °C with different crucible setups

Run	Ash (mg)	Graphite surface-to-ash ratio (cm^2/g)	Whiskers
Alumina crucible and lid	1900	–	No whiskers
Graphite—low ratio	2100	20	Si_2N_2O
Graphite—standard ratio	170	50	Si_2N_2O
Graphite—high ratio	300	150	α-Si_3N_4

All whiskers were found to be deposited preferentially on graphite surfaces and had lengths in the millimeter range. While Si_2N_2O whisker diameters varied from about 100 to 500 nm, Si_3N_4 whiskers had rectangular cross sections varying between 100 nm and 1 µm. However, Si_3N_4 whiskers obtained from the ash appeared thinner and not as well developed when compared to the corresponding ones obtained from husk as the starting material at the same soaking temperature value of 1400 °C (see Fig. 11).

The experimental observation that high graphite surface-to-ash ratios in the experimental setup led to silicon nitride whiskers may suggest that the rate-limiting step for full nitridation may be the carbothermal reduction reaction rather than the nitridation step (see Eq. 3).

4 Conclusions

Rice husk and as-produced rice husk ash from a local cogeneration plant, without any pretreatments, were employed as starting materials to readily produce silicon nitride and silicon oxynitride whiskers by carbothermal reduction and nitridation. α-silicon nitride whiskers were obtained when rice husk was used, while α-silicon oxynitride whiskers were the predominant product observed for the industrial ash. Rice husk resulted in a more substantial whisker development when compared to the ash for all temperatures evaluated. For both starting materials, increasingly vigorous reaction rates were observed with increasing soaking temperatures, with the overall best results observed at 1400 °C. Graphite crucibles promoted a more substantial whisker development for the husk, and a high graphite crucible surface-to-ash ratio setup enabled the production of α-silicon nitride whiskers from the ash. α-silicon nitride whiskers had square or

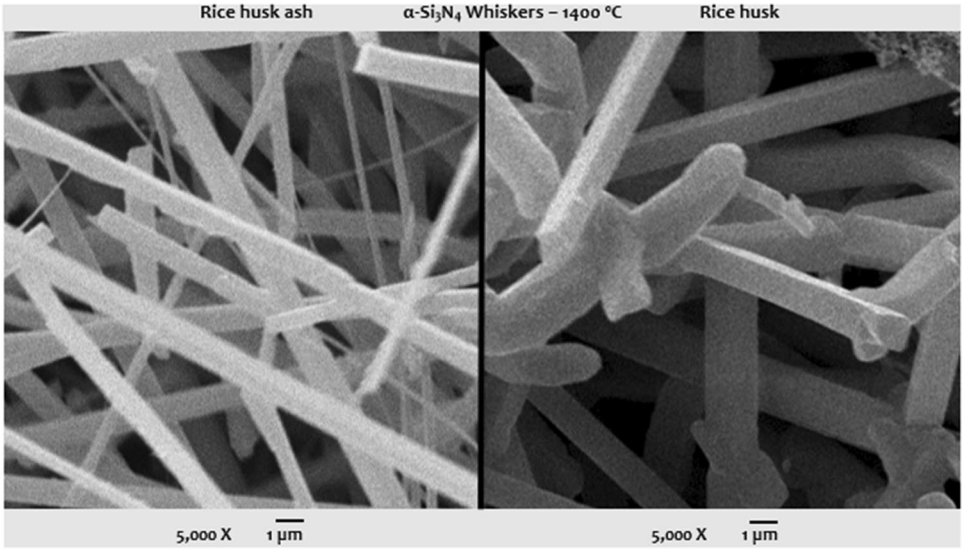

Fig. 11 SEM SE images of α-Si_3N_4 whiskers developed with a high-ratio graphite crucible setup for industrial rice husk ash at the soaking temperature of 1400 °C. The SEM micrograph of α-Si_3N_4 whiskers obtained from rice husk in a graphite crucible at 1400 °C has been included for comparison purposes

rectangular cross sections ranging from about 100 nm up to 1 µm, whereas silicon oxynitride whiskers had cross sections ranging from about 100 nm up to 500 nm. Both types of whiskers had lengths in the millimeter range. Throughout the different runs, whiskers grew much more preferentially on the crucible and lid surfaces when compared to the residue leftover from the starting materials, a fact that may aptly enable whisker recovery with a different experimental setup by crystallizing the products separately from the reaction chamber.

Acknowledgments The authors would like to thank Departamento Ingeniería de Materiales y Minas, Instituto de Ingeniería Química, Facultad de Ingeniería, UdelaR, for providing the financial support and experimental facilities required to carry out this work.

Funding The funding required for this work was provided by Departamento Ingeniería de Materiales y Minas, Instituto de Ingeniería Química, Facultad de Ingeniería, UdelaR.

Compliance with ethical standards

Conflicts of interest The authors declare that they have no conflict of interest.

References

1. Soltani N, Bahrami A, Pech-Canul M, González L (2015) Review on the physicochemical treatments of rice husk for production of advanced materials. Chem Eng J 264:899–935. https://doi.org/10.1016/j.cej.2014.11.056
2. Hossain S, Mathur L, Roy P (2018) Rice husk/rice husk ash as an alternative source of silica in ceramics: review. J Asian Ceram Soc 6:299–313. https://doi.org/10.1080/21870764.2018.1539210
3. Soltani N, Soltani S, Bahrami A, Pech-Canul M, González L, Möller A, Tapp J, Gurlo A (2017) Electrical and thermomechanical properties of CVI- Si_3N_4 porous rice husk ash infiltrated by Al–Mg–Si alloys. J Alloys Compd 696:856–868. https://doi.org/10.1016/j.jallcom.2016.12.051
4. Bahrami A, Schierning G, Nielsch K (2020) Waste recycling in thermoelectric materials. Adv Energy Mater. https://doi.org/10.1002/aenm.201904159
5. Soltani N, Bahrami A, Pech-Canul M, González L (2019) Improving the interfacial reaction between cristobalite silica from rice husk and Al–Mg–Si by CVD-Si_3N_4 deposition. Waste Biomass Valoriz 11:3789–3799. https://doi.org/10.1007/s12649-019-00706-w
6. Pierson HO (1996) Handbook of refractory carbides and nitrides: properties, characteristics, processing, and applications. Noyes Publications, Park Ridge, NJ
7. Weimer AW (1997) Carbide, nitride, and boride materials synthesis and processing. Chapman & Hall, London
8. Riedel R, Chen I-W (2015) Ceramics science and technology. Wiley, Weinheim
9. Padhi B, Patnaik C (1995) Development of Si_2N_2O, Si_3N_4 and SiC ceramic materials using rice husk. Ceram Int 21:213–220. https://doi.org/10.1016/0272-8842(95)90912-3
10. Bengisu M (2001) Engineering ceramics. Springer, Berlin
11. Qadri S, Rath B, Gorzkowski E, Wollmershauser J, Feng C (2016) Nanostructured silicon nitride from wheat and rice husks. J Appl Phys 119:134902. https://doi.org/10.1063/1.4945391
12. Pavarajarn V, Precharyutasin R, Praserthdam P (2010) Synthesis of silicon nitride fibers by the carbothermal reduction and nitridation of rice husk ash. J Am Ceram Soc 93:973–979. https://doi.org/10.1111/j.1551-2916.2009.03530.x
13. Patel M, Prasanna P (1993) Formation of SiC and Si_2N_2O from acid-treated rice husk with catalysts. Trans Indian Ceram Soc 52:172–175. https://doi.org/10.1080/0371750x.1993.10804598
14. Cutler IB (1974) Production of silicon nitride from rice hulls. U. S. Patent 3,855,395, 17 December, 1974
15. Rahman I (1994) Preparation of Si_3N_4 by carbothermal reduction of digested rice husk. Ceram Int 20:195–199. https://doi.org/10.1016/0272-8842(94)90039-6
16. Real C, Alcalá M, Criado J (2004) Synthesis of silicon nitride from carbothermal reduction of rice husks by the constant-rate-thermal-analysis (CRTA) method. J Am Ceram Soc 87:75–78. https://doi.org/10.1111/j.1551-2916.2004.00075.x
17. Ali M, Tindyala M (2015) Thermoanalytical studies on acid-treated rice husk and production of some silicon based ceramics from carbonised rice husk. J Asian Ceram Soc 3:311–316. https://doi.org/10.1016/j.jascer.2015.06.003
18. Rahman I (1998) The formation of different Si_3N_4 phases in the presence of V_2O_5 during carbothermal reduction of untreated and acid treated rice husk. Ceram Int 24:293–297. https://doi.org/10.1016/s0272-8842(97)00014-x
19. Rahman I, Riley F (1989) The control of morphology in silicon nitride powder prepared from rice husk. J Eur Ceram Soc 5:11–22. https://doi.org/10.1016/0955-2219(89)90004-6
20. Neto E, Kiminami R (2014) Synthesis of silicon nitride by conventional and microwave carbothermal reduction and nitridation of rice hulls. Adv Powder Technol 25:654–658. https://doi.org/10.1016/j.apt.2013.10.009
21. Sarangi M (2009) Effect of an iron catalyst and process parameters on Si-based ceramic materials synthesized from rice husks. Silicon 1:103–109. https://doi.org/10.1007/s12633-009-9015-1
22. Kuskonmaz N, Sayginer A, Toy C, Acma E, Addemir O, Tekin A (1996) Studies on the formation of silicon nitride and silicon carbide from rice husk. High Temp Mater Process 15:123–128. https://doi.org/10.1515/htmp.1996.15.1-2.123
23. Real C, Córdoba J, Alcalá M (2018) Synthesis and characterization of SiC/Si_3N_4 composites from rice husks. Ceram Int 44:14645–14651. https://doi.org/10.1016/j.ceramint.2018.05.090
24. Liou T-H, Chang F-W (1996) The nitridation kinetics of pyrolyzed rice husk. Ind Eng Chem Res 35:3375–3383. https://doi.org/10.1021/ie950222j
25. Yuan W, Fan M, Deng C et al (2015) The phase-formation behavior of composite ceramic powders synthesized by utilizing rice husk ash from the biomass cogeneration plant. Adv Mater Sci Eng 2015:1–7. https://doi.org/10.1155/2015/376151
26. Zawrah M, Zayed M, Ali M (2012) Synthesis and characterization of SiC and SiC/Si_3N_4 composite nano powders from waste material. J Hazard Mater 227–228:250–256. https://doi.org/10.1016/j.jhazmat.2012.05.048

27. Stuart B (2004) Infrared spectroscopy: fundamentals and applications. Wiley, Chichester
28. Nyquist R, Kagel R (1997) Infrared spectra of inorganic compounds (3800–45 cm^{-1}). Academic Press, London
29. Luongo J (1983) Infrared characterization of α- and β-crystalline silicon nitride. J Electrochem Soc 130:1560. https://doi.org/10.1149/1.2120034
30. Norris D, Rodriguez M, Fukuda S, Snyder R (1990) X-Ray powder data for α-Si_3N_4. Powder Diffr 5:225–226. https://doi.org/10.1017/S0885715600015876
31. Baraton M, Labbe J, Quintard P, Roult G (1985) L'oxynitrure de silicium: Si_2N_2O I. Attribution des absorptions du spectre infrarouge aux vibrations fondamentales. Mater Res Bull 20:1239–1250. https://doi.org/10.1016/0025-5408(85)90098-4
32. Larker R (1992) Reaction sintering and properties of silicon oxynitride densified by hot isostatic pressing. J Am Ceram Soc 75:62–66. https://doi.org/10.1111/j.1151-2916.1992.tb05442.x